Available online at www.sciencedirect.com
ScienceDirect
International Journal of Hydrogen Energy 32 (2007) 2957–2964
International Journal of HYDROGEN ENERGY
www.elsevier.com/locate/ijhydene

Simulation of heat transfer in a metal hydride reactor with aluminium foam

F. Laurencelle*, J. Goyette

Institut de recherche sur l'hydrogène, Université du Québec à Trois-Rivières, 3351 Boul. Des Forges, CP 500, Trois-Rivières, Canada G9A 5H7

Received 7 November 2006; received in revised form 13 December 2006; accepted 14 December 2006
Available online 9 February 2007

Abstract

A 1-D model has been developed to evaluate various designs of metal hydride reactors with planar, cylindrical or spherical geometry. It simulates a cycling loop (absorption–desorption) focusing attention on the heat transfer inside the hydride bed, which is considered the rate-limiting factor. We have validated this model with experimental data collected on two reactors, respectively, containing 1 and 25 g of $LaNi_5$, the second being equipped with aluminium foam. The simulation program reproduces accurately our experimental results. The impact of the foam cell size has been studied. According to our model, the use of aluminium foam allows the reactor diameter to be increased by 7.5 times, without losing its performance.

Keywords: Hydrogen storage materials; Heat transfer; Simulation; Aluminium foam; Reaction kinetics; Metal hydrides

1. Introduction

Metal-hydride systems have become a secure and effective way to store hydrogen for fuel cells and to produce thermodynamic or electrochemical work for stationary and mobile applications [1–4]. Indeed, they reach the highest volumetric capacity of all hydrogen storage techniques and new hydride compounds are currently being developed to enhance their gravimetric storage ability [5]. The heat energy exchanged during the absorption and desorption processes is quite large (near −30.8 kJ per mole of hydrogen gas for $LaNi_5$ [6] hydride and −75.0 for MgH_2 [7] and the metal hydride reactor should manage this heat to prevent inhibiting reaction. Several experimental studies on hydride powder beds or compacted mixtures have been carried out to determine the limit reaction rate that corresponds to a nearly isothermal process [8,9]. They show that, in AB_5 hydrides, the intrinsic reaction kinetics is very fast but the heat transfer controls the overall reaction rate. In fact, because metal hydrides have a low thermal conductivity (around 0.1 W/m K for AB_5 powders [10]), it is often necessary to include an additional heat transfer material inside the hydride bed, such as metal foam. In a previous publication [11], we have described the design of a hydride reactor equipped with an aluminium foam; it is now used in a hydrogen compression device. Since then, we have developed a computer program that simulates the behaviour of planar, cylindrical or spherical hydride reactors. The first simulation results are in agreement with our experimental data and we have now the opportunity to explore new designs of reactors. Thus, the objectives of this work are to show the impact of the aluminium foam used to enhance the hydride reaction and to evaluate by simulation the dimension limits of an efficient reactor design.

We have programmed our simulation software in *Borland Delphi* 2005 (object oriented Pascal), which operates under *Microsoft Windows XP*. It contains a tool for editing the parameters and it can present the results in graphs or save them in text files. The experimental set-up, a volumetric titration system, evaluates all hydrogenation properties of hydride samples: i.e. PCT curves, activation, thermodynamics, kinetics and cycling behaviour. It computes the hydrogen absorbed/desorbed by following the pressure changes in known constant volumes (Sieverts' method). We have characterized two reactors for this study. The smallest one is a $\frac{1}{4}$ in *Swagelok VCR* part having one of its ends capped. The largest is a closed-end tube machined in an aluminium piece connected with $\frac{1}{2}$ in *VCR* fittings.

* Corresponding author. Tel.: +1 819 376 5108; fax: +1 819 376 5164.
E-mail address: francois.laurencelle@uqtr.ca (F. Laurencelle).

0360-3199/$ - see front matter © 2007 International Association for Hydrogen Energy. Published by Elsevier Ltd. All rights reserved.
doi:10.1016/j.ijhydene.2006.12.007

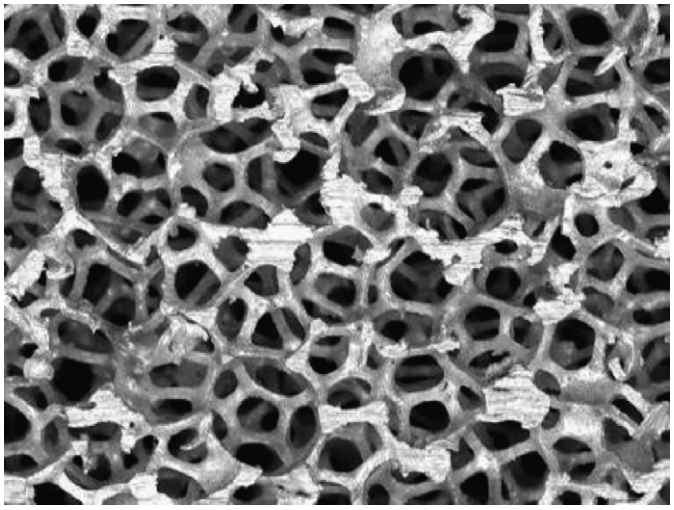

Fig. 1. Enlarged view of a 40 ppi foam.

A *Duocel* aluminium foam from *ERG Materials and Aerospace Corporation* [12] is press-fitted inside the reactor. This foam has a random open-cell structure (see Fig. 1). In this paper, we propose to model a typical cell of this foam as a sphere.

2. Model description

The model computes heat transfers in one dimension (say r) by the finite difference method. We start with the heat equation:

$$\frac{\partial(\rho c_p T)}{\partial t} = \frac{\partial}{\partial r}\left(k_{\text{eff}}\frac{\partial T}{\partial r}\right) + S''', \tag{1}$$

where the source term S''' is decomposed in two parts for solving purposes:

$$S''' = S'''_C + S'''_P T. \tag{2}$$

The simulation domain, e.g. the whole reactor or a part of it, is represented by an array of 1 to N cells along the radius r. The boundary conditions are set at both ends of the domain, in two extra cells with indices 0 and $N+1$. Fig. 2 shows the structure of the domain.

The variables r_{i-} and r_{i+} are, respectively, the left and right positions of the walls of a given mesh (indexed i), while A_{i-} and A_{i+} are the surfaces normal to the heat flow at those positions.

The finite difference method gives a temperature value for each mesh i. We use the fully implicit formulation [13,14], wherein the temperature values T_i, except T_i^0, are the anticipated values at the end of the current time step:

$$(\rho c_p)_i V_i \frac{T_i - T_i^0}{\Delta t} = a_{i-}T_{i-1} + a_{i+}T_{i+1} - (a_{i-} + a_{i+})T_i + S'''_{Ci}V_i + S'''_{Pi}V_i T_i, \tag{3}$$

where

$$a_{i+} = \frac{1}{\int_{r_i}^{r_{i+1}} (1/k_{\text{eff}}A(r))\,\mathrm{d}r} \approx \frac{k_{\text{eff}}A_{i+}}{r_{i+1} - r_i} \tag{4}$$

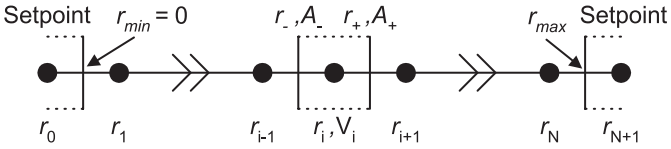

Fig. 2. Schema of the simulated domain.

and

$$a_{i-} = \frac{1}{\int_{r_{i-1}}^{r_i} (1/k_{\text{eff}}A(r))\,\mathrm{d}r} \approx \frac{k_{\text{eff}}A_{i-}}{r_i - r_{i-1}}. \tag{5}$$

So

$$T_i = \frac{((\rho c_p)_i V_i T_i^0/\Delta t) + a_{i-}T_{i-1} + a_{i+}T_{i+1} + S'''_{Ci}V_i}{((\rho c_p)_i V_i/\Delta t) + a_- + a_+ - S'''_{Pi}V_i}. \tag{6}$$

The last equation is solved with the Gauss–Siedel algorithm [13,14] with five iterations per time step.

The density of each material present in the reactor is weighed taking into account the porosities ε.

$$\rho_{\text{foam}} = (1 - \varepsilon_{\text{foam}})\rho_{\text{foam[bulk]}}, \tag{7}$$

$$\rho_{\text{M}} = \varepsilon_{\text{foam}}(1 - \varepsilon_{\text{MH}})\rho_{\text{M[bulk]}}, \tag{8}$$

$$\rho_{\text{H}} = x_{\text{H}} C_{\text{MH}} \rho_{\text{M}}, \tag{9}$$

$$\rho_{\text{H}_2} = \varepsilon_{\text{foam}}\varepsilon_{\text{MH}} M_{\text{H}_2} \frac{p_{\text{g}}}{R_{\text{g}} T_{\text{rea}}}, \tag{10}$$

where x_{H}, which can take values between 0 and 1, is the fraction of the maximal hydrogen loading capacity C_{MH} in a given mesh. M_{H_2} is the molecular mass of H_2.

The coefficient ρc_p in the heat transfer equations is a composite parameter:

$$\rho c_p = \rho_{\text{foam}} c_{p\text{foam}} + (\rho_{\text{M}} + \rho_{\text{H}}) c_{p\text{MH}} + \rho_{\text{H}_2} c_{p\text{H}_2} \tag{11}$$

and the effective thermal conductivity is

$$k_{\text{eff}} = k_{\text{foam}} + \varepsilon_{\text{foam}} k_{\text{MH}} + \varepsilon_{\text{foam}}\varepsilon_{\text{MH}} k_{\text{H}_2}. \tag{12}$$

If there is no foam in the reactor, $k_{\text{foam}} = 0$ and $\varepsilon_{\text{foam}} = 1$.

The pressure composition isotherm (PCT) reflects the phase diagram of the hydrogen–metal reaction. At a given temperature, the difference between the hydrogen gas pressure and the equilibrium plateau pressure of the hydride controls the reaction rate. According to the van't Hoff relation, the plateau pressure of an ideal hydride depends only on the temperature. Nonetheless, we have added a constant slope term to approximate the behaviour of a real material. Then, the equilibrium pressure $p_{\text{eq},r}$ is a function of the temperature T and hydrogen concentration x_{H}:

$$y = \ln\left(\frac{p_{\text{eq},r}}{1\ \text{atm}}\right) = \frac{\Delta H_r}{R_{\text{g}} T} - \frac{\Delta S_r}{R_{\text{g}}} + g_r\left(x_{\text{H}} - \frac{1}{2}\right), \tag{13}$$

where index r denotes either the absorption (abs) or desorption (des) reaction and g_r is the plateau slope.

The reaction kinetic equations are taken from [15–18], where $p_{eq,abs}$ and $p_{eq,des}$ are computed from Eq. (13):

Absorption:

$$\frac{dx_H}{dt} = k_{abs} \exp\left(-\frac{E_{abs}}{R_g T}\right) \ln\left(\frac{p_g}{p_{eq,abs}}\right)(1 - x_H), \quad (14)$$

Desorption:

$$\frac{dx_H}{dt} = k_{des} \exp\left(-\frac{E_{des}}{R_g T}\right)\left(\frac{p_g - p_{eq,des}}{p_{eq,des}}\right) x_H. \quad (15)$$

The heat source terms S'''_{Ci} and S'''_{Pi} are computed from

$$S'''_i = S'''_{Ci} + S'''_{Pi} T_i = \left(\frac{d\rho_H}{dt}\right)_i \left[-\frac{\Delta H_r}{M_{H_2}} + (c_{pMH} - c_{pH_2}) T_i\right], \quad (16)$$

which includes the heat balance from the local phase transformation.

According to the simulations of [15], hydrogen diffusion is much faster than heat transfer. Therefore, we consider a uniform pressure field with no gradient and instantaneous diffusion. So, the overall pressure (in the preset system volume and the free volume inside the hydride reactor) is updated at each time step using the total gas balance in the reactor and system volumes (V_{rea} and V_{sys}):

$$N_g = \frac{p_g}{R_g}\left(\frac{V_{sys}}{T_{sys}} + \frac{V_{rea}}{T_{rea}}\right) + \frac{\Delta t}{M_{H_2}} \sum_{i=1}^{N} \left(\frac{d\rho_H}{dt}\right)_i V_i, \quad (17)$$

$$p_g = \frac{N_g R_g}{V_{sys}/T_{sys} + V_{rea}/T_{rea}}, \quad (18)$$

where T_{rea} is the average temperature in the simulation domain:

$$T_{rea} = \frac{\sum_{i=1}^{N} (\rho c_p)_i V_i T_i}{\sum_{i=1}^{N} (\rho c_p)_i V_i}. \quad (19)$$

3. Model implementation

In order to implement the model, we have found most of the parameters describing the hydride material ($LaNi_5$) and the aluminium foam in published documents. Their values and their sources are given in Tables 1–3.

The absorption enthalpy, in Table 1, was calculated by adding the contribution of the hysteresis to the value of the desorption enthalpy, both given in Ref. [6]. Also, the hydrogenation capacity is represented by its reversible part and the curvature of the plateaux is neglected. The kinetic values in Table 2 were used in several models [15,16]. The hydride porosity, in Table 3, was estimated when filling a reactor. According to a previous publication [10], the thermal conductivity of a free powder AB_5 sample is ~ 0.1 W/m K. An aluminium foam matrix is used in our second experimental set-up. The specifications of the foam can be found in the product datasheet [19]. According to [20], the average cell diameter of a 40 ppi foam is 2.3 mm. For other foam sizes, a scale factor was applied to that value. The other parameters are common and readily available.

Table 1
PCT parameters of $LaNi_5$ [6]

Parameter	Absorption	Desorption
ΔH_r (J/mol)	−30 478	−30 800
ΔS_r (J/molK)	−108	−108
g_r (–)	0.13	0.13
C_{MH} (H/M–wt%)	1.28	1.28

Table 2
Hydrogenation kinetic properties of $LaNi_5$ [15,16]

Parameter	Absorption	Desorption
k_r (s^{-1})	59.187	9.57
E_r (J/mol)	21 170	16 420

4. Model validation

We have used two appropriate data series to validate our model. Both samples, $LaNi_5$ from Ergenics, were installed in different reactors shown in Fig. 3 and then tested in our laboratory, with a volumetric titration system.

The first reactor, referred as "small reactor", was originally designed for the characterization of hydrides. It has an internal diameter of 6.35 mm and a length 25.4 mm. It can store 1 g of $LaNi_5$ powder and it is not equipped with any heat exchanger. The external wall of this reactor, the inlet filter and the fixation nuts, all in stainless steel, are relatively massive and they tend to keep the temperature from rapid fluctuations. During the tests, an oven with a PID controller regulates the temperature of the reactor, through an air layer, which also adversely affects the temperature regulation. A simple experiment, absorption followed by desorption, is compared with model results. The experimental conditions are given in Table 4 and Figs. 4–6 show both experiment and simulation time series.

Obviously, there is a good correlation between the experiment and the simulation data (pressure, temperature and hydrogen loading profiles). The average absorption and desorption rates in the simulation correspond very well to the experimental reaction rates. Also, the simulation reveals that the material could react more rapidly and that the large temperature variations, far away from the reactor wall, are responsible for the lagging reaction rate. Indeed, immediately after the beginning of absorption, the temperature at the centre of the reactor rises 40 °C above the set point, due to the poor heat transfer capability of the hydride powder (a similar effect is observed at desorption). The controller has difficulty in maintaining a constant temperature on the reactor wall, so that it varies by about ±10 °C around the set point. Nonetheless, the reactor wall may not be the best location to measure the temperature because it constitutes a thermal ballast [9]. However, this has a smaller impact on the reaction rate than the temperature variations inside the reactor .

The second reactor, identified as "large reactor", was machined in an aluminium piece with VCR connectors: it is a tube with an internal diameter of 12.7 mm and a length of 76.2 mm.

Table 3
Physical properties of the components of the reactor

	Al foam	$LaNi_5$	H_2 (gas)
Density (kg/m^3)	$\rho_{foam[bulk]} = 2700$	$\rho_{M[bulk]} = 8310$	—
Porosity (–)	$\varepsilon_{foam} = 0.91$ [19]	$\varepsilon_{MH} = 0.55$	—
Spec. heat (J/kg K)	$c_{pfoam} = 963$	$c_{pMH} = 355$ [10]	$c_{pH_2} = 14\,266$
Th. cond. (W/m K)	$k_{foam} = 10.9$ [19]	$k_{MH} = 0.1$ [10]	$k_{H_2} = 0.1897$

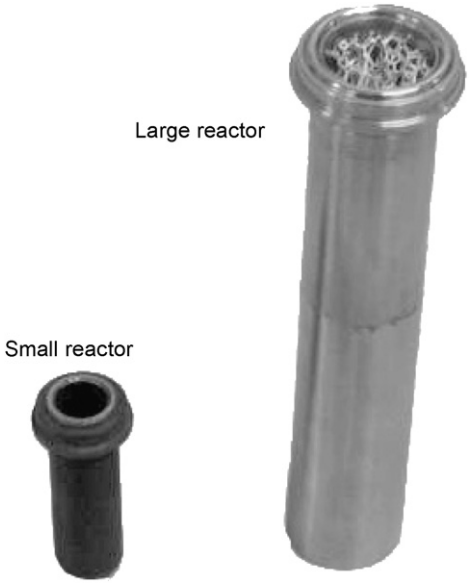

Fig. 3. Hydride reactors used for model validation.

Table 4
Simulation and experimental conditions: "small reactor"

Parameter	Value
Geometry	Cylindrical
Radius r_{max} (mm)	3.175
Height h (mm)	25.40
ε_{foam} (–)	1 (no foam)
ε_{MH} (–)	0.55
$LaNi_5$ M_M (g)	1.000
Reactor V_{rea} (ml)	7.05
T_{sys} (°C)	25
T_{abs} (°C)	23
T_{des} (°C)	23
$V_{sys[abs]}$ (ml)	129
$V_{sys[des]}$ (ml)	588
p_{abs} (atm)	5.956
p_{des} (atm)	0.068

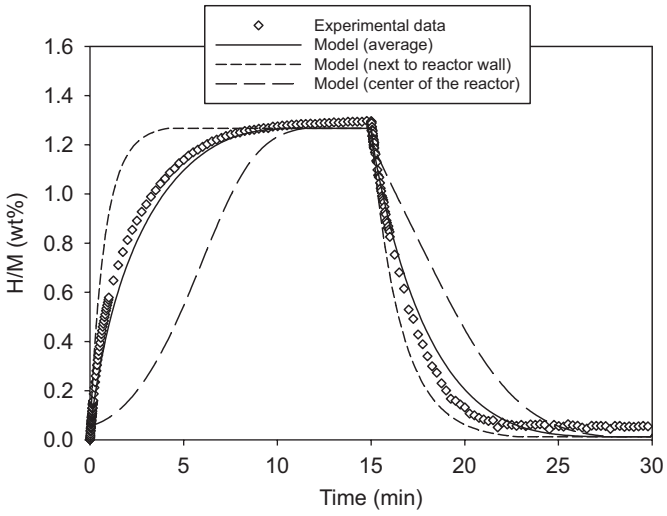

Fig. 4. Small reactor: hydrogenation profiles.

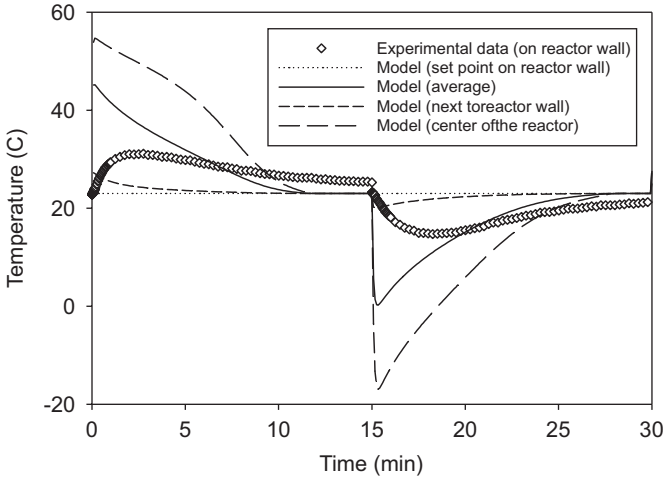

Fig. 5. Small reactor: temperature profiles.

A 40 ppi (pores per inch) aluminium foam, press-fitted inside, improves the heat transfer rate. This reactor can contain 25 g of $LaNi_5$ powder and its aluminium shell and foam weight only 18 g. It was designed for a hydrogen compressor with two set points between 15 and 85 °C. A water circulation loop insures the thermal regulation more efficiently than with the preceding design for 1 g of hydride. There are two ways to simulate this reactor. One can calculate the effective heat capacity and thermal conductivity using Eqs. (11) and (12) and then simulate the whole reactor. Another alternative is to consider the aluminium foam as a highly efficient heat transfer material. Then, one can simulate only a metal hydride cluster, a pore in the foam, filled with hydride powder. We have run an experiment with this reactor in the conditions described in Table 5. Figs. 7 and 8 compare these results with simulation results obtained by

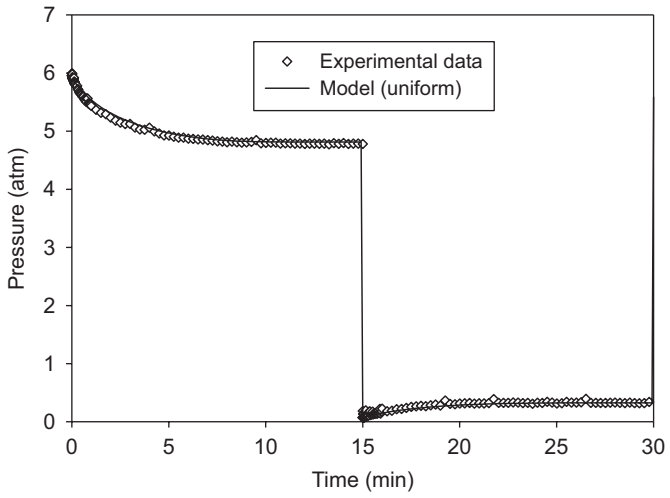

Fig. 6. Small reactor: pressure profiles.

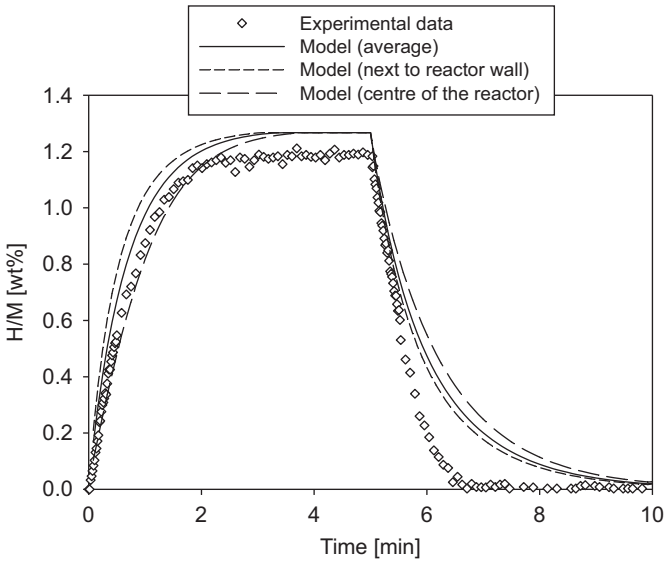

Fig. 7. Large reactor: hydrogenation profiles.

Table 5
Simulation and experimental conditions: "large reactor"

Parameter	Value	
Geometry	Cylindrical[a]	Spherical[b]
Radius r_{max} (mm)	6.35	1.15 [20]
Height h (mm)	76.20	—
ε_{foam} (–)	0.91	1 (foam pore)
ε_{MH} (–)	0.55	
$LaNi_5$ M_M (g)	25.001	
Reactor V_{rea} (ml)	59	
T_{sys} (°C)	25	
T_{abs} (°C)	50	
T_{des} (°C)	50	
$V_{sys[abs]}$ (ml)	2342	
$V_{sys[des]}$ (ml)	2342	
p_{abs} (atm)	12.73	
p_{des} (atm)	0.086	

[a]Modelling the reactor using effective heat capacity and thermal conductivity values.
[b]Modelling a spherical cluster of hydride inside a 40 ppi foam.

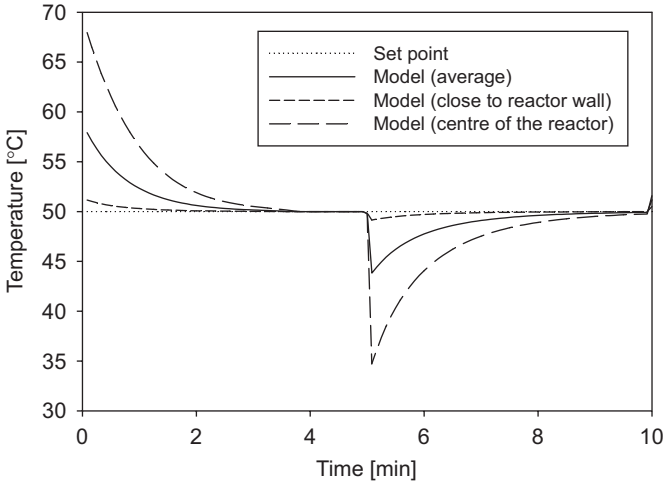

Fig. 8. Large reactor: temperature profiles.

the second method (simulation of an hydride cluster) and it can be seen that for this particular design both simulation methods give very similar results.

The absorption speed is the same in experiment and simulation, but a little discrepancy appears in the hydrogen storage capacity, which is a little smaller for the experimental data. On the other hand, the desorption reaction profiles are slightly different. Beginning with the same slope, they diverge after about 30 s. The measured desorption flow is almost constant until it stops when there is no more reactant. At the same time, the corresponding simulated curve follows nearly exponential decay. Globally, the experimental desorption rate is 1.5 times more rapid than the model predictions. In view of this information, desorption does not follow the reaction mechanism proposed in Eq. (15), which should be revised. Nonetheless, the model produces satisfactory results in most cases; hence we will use it to evaluate the theoretical limitations of some other designs of reactors.

5. Model predictions

Modelling serves as a tool to optimize the reactor design. So, looking for a system that can store more hydrogen, we have simulated larger hydride reactors, modifying their dimension and varying the size of the hydride clusters in the aluminium foam. This section describes, in three scenarios, the results of this exploratory work. The hydride material is $LaNi_5$ and the simulated operating conditions are the same as in the "large reactor" case, see Table 5, except for the controlled parameters. Based on the simulated data for absorption, we have quantified, in Table 6, the time required for half and complete reaction, and also the maximum temperature of each absorption profile that should be compared with the set point (50 °C). This is the basis of a discussion on the dimension limits of an efficient design of reactor for AB_5 hydride.

Table 6
Summary of the simulated scenarios

		Half reaction delay (s)	Complete reaction delay (s)	Temperature maximum (°C)
Reactor diameter (No foam)	2 mm	32	230	67
	4 mm	57	370	77
	6 mm	90	590	79
	8 mm	135	900	80
Reactor diameter (With foam)	1 cm	23	200	59
	2 cm	38	280	72
	4 cm	75	500	79
	6 cm	128	890	80
Foam category	40 ppi	29	220	66
	20 ppi	37	350	77
	10 ppi	100	830	79

5.1. Reactor without heat transfer material

In the first scenario, the cylindrical reactor does not contain any heat transfer material. The heat is then dissipated only through hydride powder and hydrogen gas, therefore $k_{eff} \sim 0.15$ W/m K. Figs. 9–11 show the average hydrogen loading profiles for different reactor diameters. The reaction is completed in 5 min when the diameter < 3 mm. However, if it is > 8 mm, the reaction takes more than 15 min. At the beginning of the absorption, the maximum temperature at the centre of the reactor of 8 mm of diameter is 80 °C (see Table 6). At this temperature the absorption plateau pressure is equal to the pressure setting of 12.73 atm. It therefore means that the reaction is at equilibrium until the temperature decreases due to heat conduction; see Fig. 11. In such a case, heat transfer completely controls the reaction rate [8].

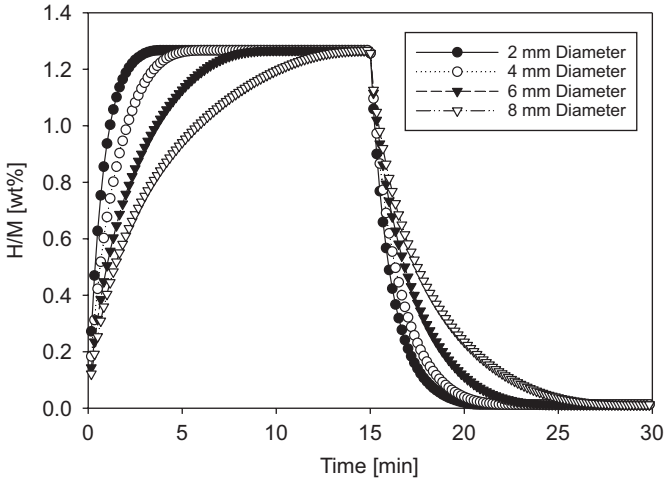

Fig. 9. No foam: average hydrogenation profiles.

5.2. Reactor with aluminium foam (91% porosity)

If the reactor is equipped with aluminium foam, like the "large reactor" in Section 3, the effective thermal conductivity can reach about 10 W/m K. A reactor having a diameter between 2.2 and 6 cm will allow the reaction to be completed between 5 and 15 min (see Fig. 12). One should note that below a few mm of reactor diameter, it is inappropriate to use the effective thermal conductivity to describe the foam/hydride/gas mixture. Also, if the foam cells are large, the simulation can overestimate the reaction speed. Despite these limitations the predictions of the model indicate a much better reaction behaviour in the presence of foam. The reactor diameter can then be increased by a factor of 7.5 while maintains similar reaction rates (compare Figs. 9 and 12).

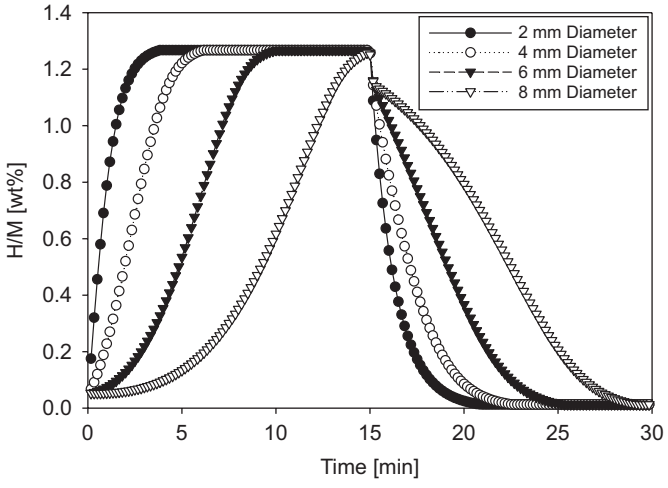

Fig. 10. No foam: hydrogenation profiles at the centre of the reactor.

5.3. Comparing different aluminium foams (10, 20 and 40 ppi)

As mentioned earlier, the efficiency of the foam to facilitate heat transfer depends on the size of its cells. We can model one cell (or hydride cluster) as a sphere filled with hydride and hydrogen gas. The average cell diameter in a 40 ppi foam is about 2.3 mm according to [20]. We have extrapolated the diameter corresponding to other foam grades (20 ppi: 4.6 mm, 10 ppi: 9.2 mm). Fig. 13 represents the results obtained when changing the foam specifications. A 5 min reaction can be obtained when the foam cell diameter is below 4 mm (> 20 ppi). We do not

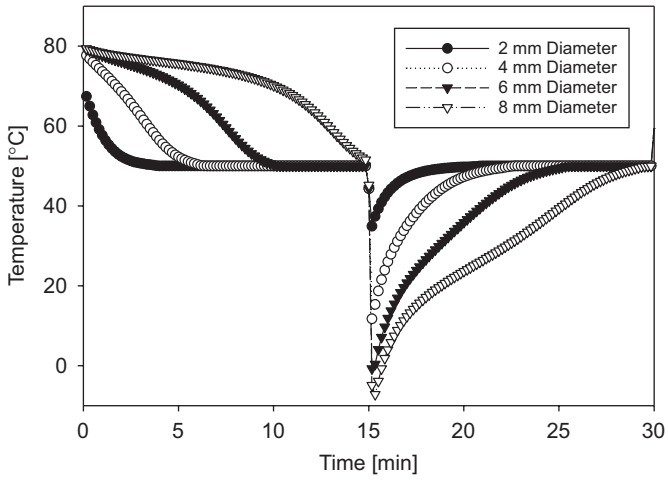

Fig. 11. No foam: temperature profiles at the centre of the reactor.

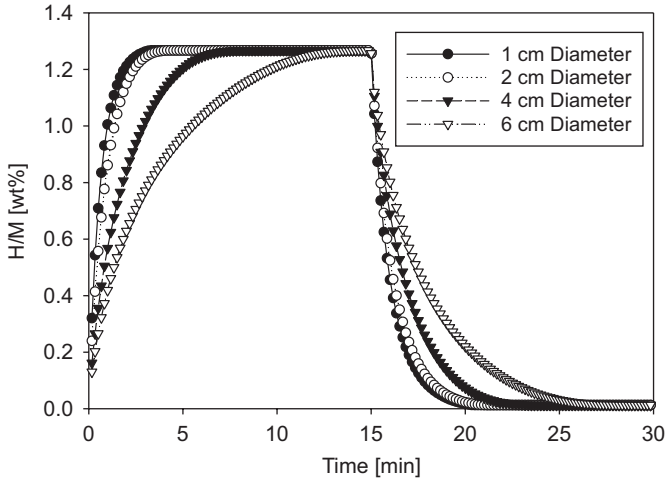

Fig. 12. With foam: average hydrogenation profiles.

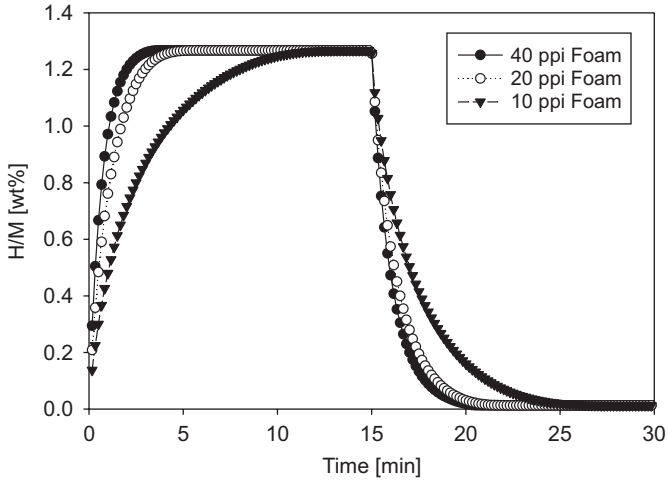

Fig. 13. Different foams: hydrogenation profiles.

recommend using the 10 ppi foam (15 min reaction) in hydride reservoirs. It is important to mention that the hydride reaction in a reactor with foam depends on two major heat transfer resistances: conduction inside the foam cells and along the path to the reactor wall, i.e. inside the foam/hydride/gas medium.

6. Conclusion

We have developed a simulation software predicting the heat flow and the reaction speed of metal hydrides in a reactor section represented by a 1-D geometry. The reservoir can include an internal heat exchanger like aluminium foam. The model is validated by comparison with two sets of experimental data. The results are in an acceptable range and give us information about the real temperature behaviour at different points of the reactors used in experiments. However, the modelled kinetics for desorption appear slightly slower than the experiments. The modelling equation for desorption seems not perfectly adapted to the reaction type. Also, our $LaNi_5$ samples may not behave (plateaux or activation state) like the one that served to implement the kinetic model [21]. The difference between the random structure of real foams and the simulated idealized foam does not seem problematic. However, in a future version of the model, optimization could be performed by mixing different heat transport phenomena and by adding gas diffusion. We have shown that a reservoir without heat exchanger must be small (less than 8 mm of diameter) to allow a fast reaction (< 15 min). If the reservoir contains an aluminium foam, this limit can be extended to a diameter of 6 cm. Also, a foam grade of < 20 ppi is not effective and not recommended, because the heat transport inside a hydride cluster would seriously reduce the reaction rate. Then, a reservoir with a 40 ppi foam, with a diameter of 4 cm and a height of 15 cm, containing about 500 g of alloy, would complete the reaction in less than 15 min, if the heat is properly conducted away its external wall. For larger reactors, one would need to allow for the mass transfer limits too. It is planned to simulate reactors containing other hydride materials such as magnesium or complex hydrides.

Acknowledgement

This work has been realized with the support of Natural Resource Canada (NRCan), Fonds Québécois de la Recherche sur la Nature et les Technologies (FQRNT) and Natural Sciences and Engineering Research Council (NSERC) of Canada.

References

[1] Sandrock G, Bowman Jr. RC. Gas-based hydride applications: recent progress and future needs. J Alloys Compd 2003;356–357:794–9.
[2] Eberle U, Arnold G, von Helmolt R. Hydrogen storage in metal-hydrogen systems and their derivatives. J Power Sources 2006;154:456–60.
[3] Feng F, Geng M, Northwood DO. Electrochemical behaviour of intermetallic-based metal hydrides used in Ni/metal hydride (MH) batteries: a review. Int J Hydrogen Energy 2001;26:725–34.
[4] Groll M, Klein HP. Metal hydride technology with special emphasis on thermodynamic machines. Fifth ISHMT-ASME heat & mass transfer conference, Calcutta, January 3–5 2002.

[5] Züttel A, Wenger P, Sudan P, Mauron P, Orimo SI. Hydrogen density in nanostructured carbon, metals and complex materials. Mater Sci Eng 2004;B108:9–18.
[6] Sandrock G. A panoramic overview of hydrogen storage alloys from a gas reaction point of view. J Alloys Compd 1999;293–295:877–88.
[7] Kapischke J, Hapke J. Measurement of the effective thermal conductivity of a Mg-MgH_2 packed bed with oscillating heating. Exp Therm Fluid Sci 1998;17:347–55.
[8] Goodell PD, Sandrock GD, Huston L. Kinetics and dynamic aspects of rechargeable metal hydrides. J Less Common Met 1980;73:135–42.
[9] Ron M, Josephy Y. Dynamic characteristics of the hydrogen sorption process in $MmNi_{4.15}Fe_{0.85}H_x$ compacts. J Less Common Met 1987;131:51–9.
[10] Dehouche Z, Grimard N, Laurencelle F, Goyette J, Bose TK. Hydride alloys properties investigations for hydrogen sorption compressor. J Alloys Compd 2005;399:224–36.
[11] Laurencelle F, Dehouche Z, Goyette J, Bose TK. Integrated electrolyser-metal hydride compression system. Int J Hydrogen Energy 2006;31:762–8.
[12] ERG Materials and Aerospace Corporation. ⟨URL:www.ergaerospace.com⟩.
[13] Patankar SV. Numerical heat transfer and fluid flow. New York: Hemisphere/McGraw-Hill; 1980 197pp.
[14] Incropera FP, DeWitt DP. Fundamentals of heat and mass transfer. Fifth ed., New York: Wiley; 2002 1008pp.
[15] Askri F, Jemni A, Nasrallah SB. Prediction of heat and mass transfer in a closed metal-hydrogen reactor. Int J Hydrogen Energy 2004;29:195–208.
[16] Askri F, Jemni A, Nasrallah SB. Study of two-dimensional and dynamic heat and mass transfer in a metal–hydrogen reactor. Int J Hydrogen Energy 2003;28:537–57.
[17] Mayer U, Groll M, Supper W. Heat and mass transfer in metal hydride reaction beds: experimental and theoretical results. J Less Common Met 1987;131:235–44.
[18] Mat MD. Numerical study of hydrogen absorption in an Lm-Ni_5 hydride reactor. Int J Hydrogen Energy 2001;26:957–63.
[19] Duocel Aluminum Foam. ⟨URL:www.ergaerospace.com/literature/erg_duocel.pdf⟩.
[20] Boomsma K. Metal foams as compact high performance heat exchangers. Mech Mater 2003;35:1161–76.
[21] Suda S, Kobayashi N, Yoshida K. Reaction kinetics of metal hydrides and their mixtures. J Less Common Met 1980;73:119–26.